

Lawrence Berkeley National Laboratory

Lawrence Berkeley National Laboratory

Title

Benchmark of the IMPACT Code for High Intensity Beam Dynamics Simulation

Permalink

<https://escholarship.org/uc/item/10h5h1qx>

Authors

Qiang, J.
Ryne, R.D.

Publication Date

2008-05-27

1.1 Benchmark of the IMPACT Code for High Intensity Beam Dynamics Simulation

J. Qiang and R. D. Ryne

mail to: jqiang@lbl.gov

[Lawrence Berkeley National Laboratory](http://www.lbl.gov), Berkeley, CA 94720, USA

1.1.1 Introduction

The IMPACT (Integrated Map and Particle Accelerator Tracking) code was first developed under Computational Grand Challenge project in the mid 1990s [1]. It started as a three-dimensional (3D) data parallel particle-in-cell (PIC) code written in High Performance Fortran. The code used a split-operator based method to solve the Hamiltonian equations of motion. It contained linear transfer maps for drifts, quadrupole magnets and rf cavities. The space-charge forces were calculated using an FFT-based method with 3D open boundary conditions and longitudinal periodic boundary conditions. This code was completely rewritten in the late 1990s based on a message passing parallel programming paradigm using Fortran 90 and MPI following an object-oriented software design. This improved the code's scalability on large parallel computer systems and also gave the code better software maintainability and extensibility [2]. In the following years, under the SciDAC-1 accelerator project, the code was extended to include more accelerating and focusing elements such as DTL, CCL, superconducting linac, solenoid, dipole, multipoles, and others. Besides the original split-operator based integrator, a direct integration of Lorentz equations of motion using a leap-frog algorithm was also added to the IMPACT code to handle arbitrary external nonlinear fields. This integrator can read in 3D electromagnetic fields in a Cartesian grid or in a cylindrical coordinate system. Using the Lorentz integrator, we also extended the original code to handle multiple charge-state beams. The space-charge solvers were also extended to include conducting wall effects for round and rectangular pipes with longitudinal open and periodic boundary conditions. Recently, it has also been extended to handle short-range wake fields (longitudinal monopole and transverse dipole) and longitudinal coherent synchrotron radiation wake fields. Besides the parallel macroparticle tracking code, an rf linac lattice design code, an envelope matching and analysis code, and a number of pre- and post-processing codes were also developed to form the IMPACT code suite. The IMPACT code suite has been used to study beam dynamics in the SNS linac, the J-PARC linac commissioning, the CERN superconducting linac design, the Los Alamos Low Energy Demonstration Accelerator (LEDA) halo experiment, the Rare Isotope Accelerator (RIA) driver linac design, and the [FERMI@Elettra](http://www.fermilab.gov) FEL linac design [3-8]. It has also been used to study space-charge resonance in anisotropic beams [9-11].

1.1.2 Physical Model and Computational Methods

The IMPACT code assumes a quasi-static model of the beam and calculates space-charge effects self-consistently at each step together with the external acceleration and focusing fields. Here, the longitudinal distance z is used as the independent variable.

There are two macroparticle pushers: one is based on transfer maps, another is based on direct integration of the Lorentz equation.

The map based pusher uses a split-operator method to combine the techniques of magnetic optics with those of particle-in-cell simulation. In this approach, the Hamiltonian governing the motion of individual particles in the accelerator is separated into two pieces, $H=H_{\text{ext}}+H_{\text{sc}}$, where H_{ext} corresponds to externally applied fields and H_{sc} corresponds to space-charge fields. The effect of H_{ext} is treated by using map-based techniques of magnetic optics, while the effect of H_{sc} is treated by using a Poisson solver to find the scalar potential and corresponding space-charge fields that act on the beam. Let M_{ext} denote the map corresponding to H_{ext} and let M_{sc} denote the map corresponding to H_{sc} . Then the map M corresponding to $H_{\text{ext}}+H_{\text{sc}}$, accurate through second order in the step size h , is given by:

$$M(h) = M_{\text{ext}}(h/2)M_{\text{sc}}(h)M_{\text{ext}}(h/2) \quad (1)$$

Each complete step involves the following: (1) transport of a numerical distribution of particles through a half step based on M_{ext} , (2) solving Poisson's equation based on the particle positions and performing a space-charge “kick” (i.e. an instantaneous change in momenta, since H_{sc} depends only on coordinates, hence M_{sc} only affects momenta), and (3) performing transport through the remaining half of the step based on M_{ext} . An important feature of this approach is that it enables one to use large step size (i.e. large steps in the independent variable) in the regime of weak or moderate space charge. Essentially, it enables one to decouple the rapid variation of the externally applied fields from the more slowly varying space-charge fields. If more accuracy is required, one can use the fourth-order algorithm of Forest and Ruth [12] or a higher-order algorithm using a method of Yoshida [13].

The pusher based on direct integration solves the Lorentz equation using a leap-frog method. In this method, during each step, particles are drifted a half step following their current momenta, then the momenta are updated using the external fields and the space-charge forces, then the particles are drifted another half step following their new momenta. This pusher can include all details of external nonlinear acceleration and focusing fields without approximation. The disadvantage of this method is that each individual particle has to advance through the external fields with sufficient accuracy. This could result in many tiny steps in order to resolve fast oscillation of the external fields.

The space-charge forces are self-consistently computed at each step by solving the 3D Poisson equation in the beam frame. The resulting electrostatic fields are Lorentz transformed back into the laboratory frame to obtain the space-charge forces of the beam. There are presently six Poisson solvers in the IMPACT code, corresponding to transverse open or closed boundary conditions with round or rectangular shape, and longitudinal open or periodic boundary conditions. These solvers use either a spectral method for closed transverse boundary conditions, or a convolution-based Green function method for open transverse boundary conditions. The convolution for the most widely used open boundary condition Poisson solver is calculated using an FFT with doubled computational domain. The computing time of this solver scales like $N \cdot \log(N)$, where N is number of grid points. The parallel implementation is based on a two-dimensional domain decomposition approach for the three-dimensional computational domain.

1.1.3 Verification of the IMPACT code

To verify the IMPACT code, we have benchmarked this code against a time-dependent PIC code [14]. Here, the time dependent PIC code was tested using two charged particles of identical mass and opposite charges. These two particles are initially placed at the two opposite diagonal corners of a cubic box. The initial speed of the two particles is given by

$$|V| = \sqrt{\frac{q^2}{4\pi\epsilon_0 mr}} \quad (2)$$

where r is the distance from the corner of the box to the center of the box. Fig. 1 shows the rms value of position and radius of the two particles as a function of time. It is seen that the radius is independent of time since we chose the center of the orbits to be at the origin. With a right initial speed, the centrifugal force should exactly balance the static Coulomb force, and particle radius will stay constant. Using this time dependent code as baseline simulation results, we also performed a multiparticle test in which we compared the beam distribution moments through a periodic transport system of about 10 m. The first order to fourth order moments of the beam distribution together with the maximum amplitude as a function of distance are shown in Fig. 2. In this example, both simulations agree with each other very well.

Besides the above examples, the IMPACT code was also benchmarked with other codes in the European Code Comparison and Benchmarking project [15].

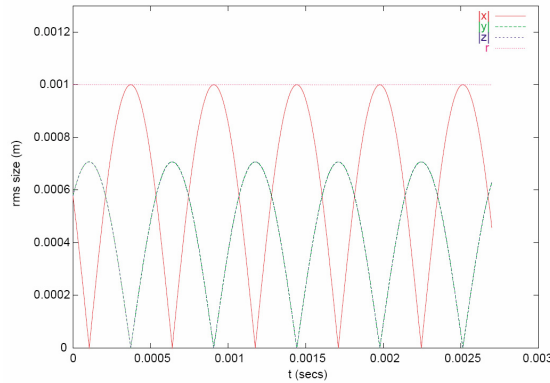


Figure 1: The position and radius of the rotating particle as a function of time.

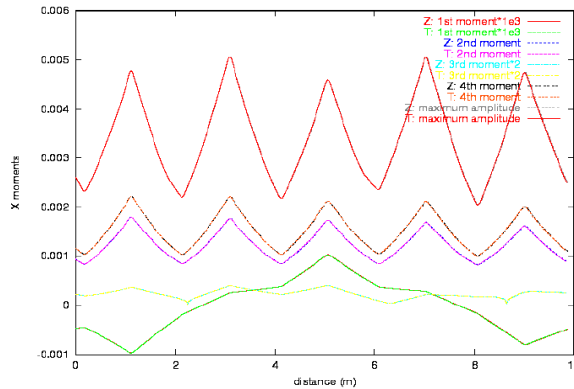


Figure 2: The first four moments and maximum amplitude as a function distance from the time-dependent PIC code and the IMPACT code.

1.1.4 Validation of the IMPACT code

The IMPACT code was also benchmarked using experimental data involving high intensity beams. Namely, we performed a comparison of simulation results and experimental results from the beam halo experiment, LEDA, at Los Alamos National Laboratory [6]. Fig. 5 shows a schematic plot of the experiment transport system after the RFQ. It consists of 52 magnetic quadrupoles with alternating polarization to provide transverse strong focusing. The beam current is 75 mA with 6.7 MeV kinetic energy. Fig. 6 shows the transverse rms size at the center of the drift space as a function of distance from the measurements and from the simulations using three types of initial distributions, Waterbag, Gaussian, and simulated RFQ output. The three distributions have the same initial Courant-Snyder parameters and emittances. Small oscillation of the measured rms sizes is reasonably reproduced from the simulation using RFQ output distribution. The emittance was determined from wire scanner measurements and compared with simulations from the IMPACT code. Fig. 7 shows the emittance from the measurements and from the simulations using the RFQ output initial distribution for a set of mismatch factors. The simulations reproduce the measurements at small mismatch factor but under-predict the emittance at large mismatch factor. This discrepancy could be due to the uncertainty of tails in the initial distribution in the experiment as compared with those used in the simulations. It was shown that a larger tail in the initial simulated distribution gives closer agreement with the measured emittance growth.

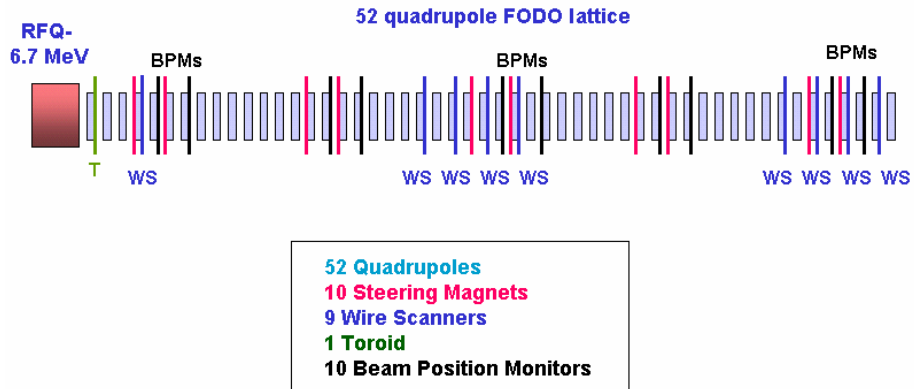


Figure 5: A schematic plot of the LEDA beam halo experiment transport system.

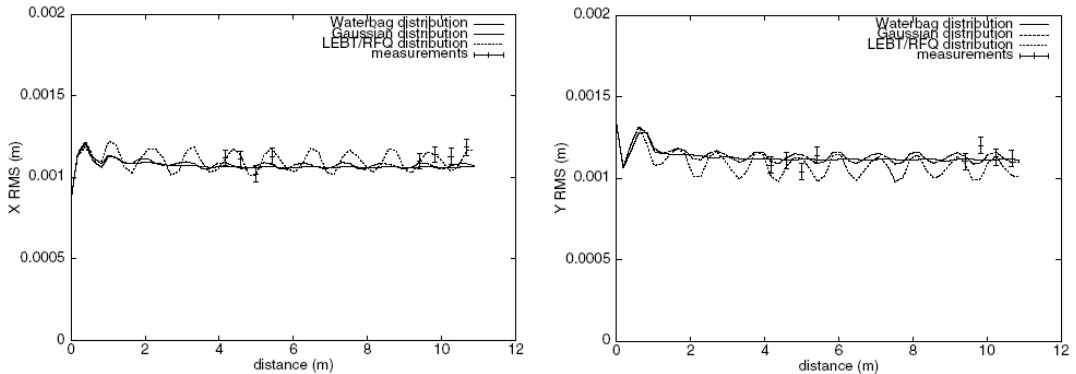


Figure 6: Horizontal and vertical rms sizes as a function of distance from the simulations and from the measurements.

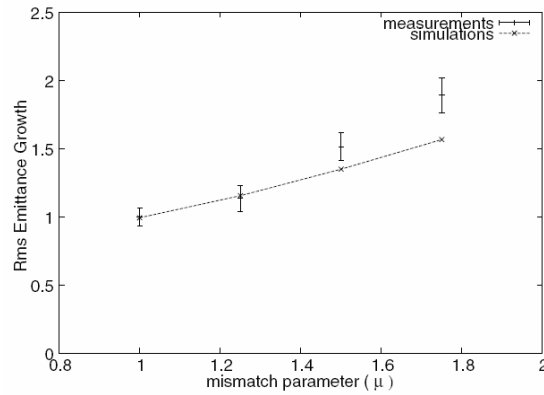


Figure 7: Final emittance growth as a function of mismatch parameter from the simulations and from the measurements.

The IMPACT code was also used to model the beam transport through a section of MEBT at the J-PARC linac [4]. Fig. 8 shows the beam profiles measured with wire scanner 3 located before quadrupole magnet 4 together with simulations from the IMPACT code. The simulated profiles show good agreement with the measured profiles with slightly less peak in the horizontal direction. The agreement in the vertical direction is excellent.

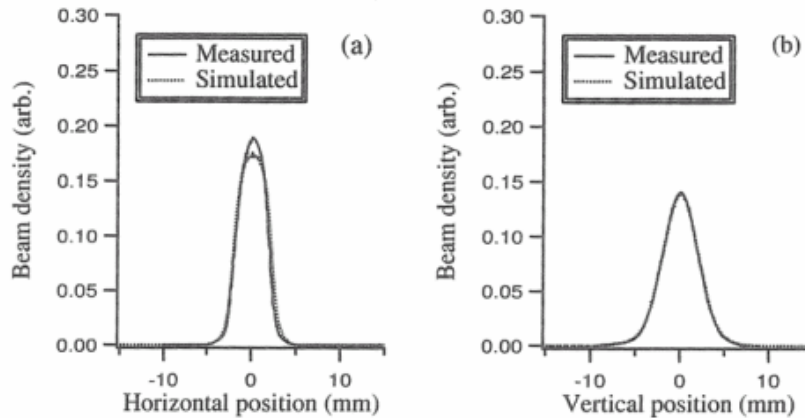


Figure 8: The measured and simulated beam density profiles in the MEBT of J-PARC linac.

1.1.5 Acknowledgements

We would like to thank Dr. S. Habib for helpful discussions during the early development of the IMPACT code, and Dr. V. Decyk for discussions about parallel implementation. We would also like to thank Dr. Tom Wangler for helpful discussions regarding the LEDA experiment, the LEDA experimental team for the validation data, and Dr. M. Ikegami for the J-PARC validation results. This work was supported by the U. S. Department of Energy under Contract no. DE-AC02-05CH11231, and by a

Scientific Discovery through Advanced Computing project, "Advanced Computing for 21st Century Accelerator Science and Technology," which is supported by the US DOE/SC Office of High Energy Physics and the Office of Advanced Scientific Computing Research. Results presented in this report were obtained using resources of the National Energy Research Scientific Computing Center, which is supported by the Office of Science of the U.S. Department of Energy under Contract No. DE-AC02-05CH11231.

1.1.6 References

1. Robert Ryne, Ji Qiang, and Salman Habib,, "Computational Challenges in High Intensity Ion Beam Physics", in "The Physics of High Brightness Beams", ed. By J. Rosenzweig and L. Serafini, World Scientific (2000).
2. J. Qiang, R. Ryne, S. Habib, V. Decyk, "An Object-Oriented Parallel Particle-In-Cell Code for Beam Dynamics Simulation in Linear Accelerators," J. Comp. Phys. vol. 163, 434, (2000).
3. J. Qiang, R. Ryne, B. Blind, J. Billen, T. Bhatia, R. Garnett, G. Neuschaefer, H. Takeda, "High Resolution Parallel Particle-In- Cell Simulation of Beam Dynamics in the SNS Linac," Nuclear Instruments and Methods in Physics Research - Section A 457, 1, (2001).
4. M. Ikegami, T. Kato, Z. Igarashi, A. Ueno, Y. Kondo, J. Qiang, and R. Ryne, "Comparison of Particle Simulation with J-PARC Linac MEBT Beam Test Results," Proc. HALO'03, May 19-23, Montauk, NY (2003).
5. F. Gerigk, M. Vretenar, R. D. Ryne, "Design of the superconducting section of the SPL linac at CERN," *Proc. PAC01*, p. 3909, (2001).
6. J. Qiang, P. L. Colestock, D. Gilpatrick, H. V. Smith, T. P. Wangler, and M. E. Schulze, "Macroparticle Simulation Studies of a Proton Beam Halo Experiment," *Phys. Rev. ST Accel. Beams*, Vol 5, 124201.
7. Robert Garnett, James Billen, Thomas Wangler, Peter Ostroumov, Ji Qiang, Robert Ryne, Richard York, Kenneth Crandall, "Advanced Beam-Dynamics Simulation Tools for RIA", *Proc. PAC2005*, Knoxville, Tennessee, May 16-20, p. 4218, (2005).
8. I.V. Pogorelov, J. Qiang, R. Ryne, M. Venturini, A. Zholents, R. Warnock, "Recent developments in IMPACT and application to future light sources," in Proc. ICAP06, Chamonix Mont-Blanc, 2006.
9. I. Hofmann, J. Qiang and R. Ryne, "Collective Resonance Model of Energy Exchange in 3D Nonequipartitioned Beams," *Physical Review Letters* 86, 2313 (2001).
10. I. Hofmann, G. Franchetti, O. Boine-Frankenheim, J. Qiang, and R. D. Ryne, "Space Charge Resonances in Two and Three Dimensional Anisotropic Beams," *Phys. Rev. ST Accel. Beams*, Vol 6. 024202 (2003).
11. J. Qiang, R. D. Ryne, I. Hofmann, "Space-charge driven emittance growth in a 3D mismatched anisotropic beam," *Phys. Rev. Lett.*, vol. 92, 174801 (2004).
12. E. Forest and R. Ruth. "Fourth-order symplectic integration," *Physica D* **43** , p. 105, (1990).
13. H. Yoshida. "Construction of higher order symplectic integrators," *Phys. Lett. A* **150** , p. 262, (1990).
14. J. Qiang, R. D. Ryne and R. W. Garnett, "Systematic comparison of position and time dependent macroparticle simulations in beam dynamics studies," *Phys. Rev. ST - Accel. Beams*, vol 5, 064201, (2002).
15. http://www-linux.gsi.de/~franchi/HIPPI/web_code_benchmarking.html.